ELSEVIER

January 1997

Materials Letters 30 (1997) 125–130

MATERIALS LETTERS

Impedance spectroscopy of SnO_2 : CoO during sintering

R. Muccillo [a,*], J.A. Cerri [b], E.R. Leite [c], E. Longo [c], J.A. Varela [d]

[a] *Instituto de Pesquisas Energéticas e Nucleares, CNEN, C.P. 11049 Pinheiros, São Paulo, S.P. 05422-970, Brazil*
[b] *Departamento de Engenharia de Materiais, Universidade Federal de San Carlos, San Carlos, S.P. 13565-905, Brazil*
[c] *Departamento de Química, Universidade Federal de San Carlos, San Carlos, S.P. 13565-905, Brazil*
[d] *Instituto de Química, Universidade Estadual Paulista, Araraquara, S.P. 14801-970, Brazil*

Received 8 July 1996; accepted 25 July 1996

Abstract

SnO_2 : m mol% CoO ($0.5 \leq m \leq 6.0$) ceramic specimens were studied by impedance spectroscopy in the 5 Hz–13 MHz frequency range during heating cold-pressed specimens from room temperature to 1250°C. The electrical resistivity during sintering decreases from 4 to 6 orders of magnitude in the 400–1500 K temperature range depending on the amount of CoO. An increase in electrical resistivity in the 570–670 K range is related to the release of adsorbed water. The results for the 970–1500 K show that the higher the amount of the CoO addition, the lower is the temperature at which SnO_2 : CoO reaches a minimum electrical resistivity. This suggests that oxygen point defects created by dissolution of cobalt ions in the SnO_2 lattice are controlling the densification rate of these ceramics.

PACS: 78.66.Li; 81.05.Je

Keywords: Tin oxide; Cobalt oxide dopant; Resistivity; Impedance spectroscopy; Dilatometry; Sintering aids

1. Introduction

Tin oxide polycrystalline ceramics are n-type semiconductors that have been widely used in humidity and carbon monoxide sensors [1,2], in thin films as crystal displays, photodetectors, solar cells and protective coatings [3–6], as electrodes for electric glass melting furnaces and for electrochromic windows [7,8]. The low densification attained by pure SnO_2 during sintering is supposed to be due to non-densifying mechanisms such as evaporation–condensation known to control mass transport during sintering, hence promoting coarsening [9–11]. SnO_2 specimens with 2 mol% CuO addition reach significant densification due to formation of a non-reactive liquid, responsible for rearrangement and an increase in lattice defect concentration causing an enhancement of mass diffusion [12,13].

Several processes and sintering aids have been used to improve SnO_2 densification [14–18]. Liquid phase sintering is the mechanism when the additives used are CuO and Bi_2O_3. MnO_2, CoO and Li_2O are additives known to form solid solutions with SnO_2. Recently, the effect of CoO and MnO_2 additions on SnO_2 sintering has been reported [11]. Using dilatometry, high temperature XRD and simultaneous thermal analysis techniques, it was found that

* Corresponding author. Fax: (55 11 8169343).

PII S0167-577X(96)00183-8

these dopants act as acceptors leading to the creation of additional oxygen vacancies in the SnO_2 lattice, resulting in an increase in the densification rate. It was also found that the addition of small amounts of CoO to SnO_2, e.g. 0.5 mol%, leads to an enhanced densification. Moreover, the onset temperature for densification decreases with the increase of dopant concentration. Considering the unusual CoO-doped SnO_2 sintering behavior [11], the electrical resistivity behavior of the SnO_2 with different amounts of CoO additions was carefully studied during sintering in order to help identify the mechanism(s) of sintering and densification of these ceramics. Electrical measurements as a function of temperature have already been used to verify whether liquid or "liquid-like" phases (i.e. along grain boundaries) are present [19]. The impedance spectroscopy (IS) technique has already been used to study polycrystalline tin oxide specimens prepared by HIP (hot isostatic pressing) and normal sintering in air *after* sintering [20]. The IS technique allows for the separation of the three main contributions to the electrical conductivity of a polycrystalline solid: bulk, internal surfaces like grain boundaries, and electrodes [21]. This is accomplished by varying the frequency of the ac input signal over a wide range in order to cover the different responses that charge carriers have inside grains, at grain boundaries and at the specimen–electrode interfaces. Here, the IS technique was used to study the electrical resistivity of SnO_2 with CoO as additive *during* and after sintering.

2. Experimental

The values of surface area, mean particle size and the degree of purity of the tin and cobalt oxides used in this study are listed in Table 1.

Both oxides SnO_2 (E. Merck) and CoO (Aldrich Chemical Co.) were separately ground in an attrition mill using yttria-stabilized zirconia balls in isopropyl alcohol as a grinding medium. Surface areas have been determined by the nitrogen gas adsorption technique (Micromeritics model ASAP 2000) by the BET method. The average particle size was calculated using the surface area value and assuming equiaxial particles. CoO (0.5 to 6 mol%) was thoroughly mixed to SnO_2 in a polyethylene jar using also yttria-stabilized zirconia in isopropyl alcohol as grinding medium. After drying, the powder was sieved in a 100 mesh screen and isostatically pressed into 1.2 cm diameter cylinders at 210 MPa. Green pellets with 57% of the theoretical density were obtained.

Table 1
Values of BET surface area, mean particle size and degree of purity of SnO_2 and CoO precursor powder oxides

Oxide	Surface area (m^2/g)	Mean particle size (μm)	Purity
SnO_2	9.2	0.09	> 99.9
CoO	3.6	0.29	> 99.0

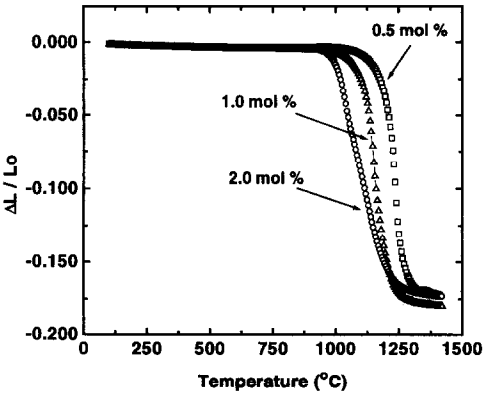

Fig. 1. Linear shrinkage as a function of temperature of SnO_2 : *m* mol% CoO (*m* = 0.5, 1.0 and 2.0) specimens.

The SnO_2 pellets containing 0.5 to 2 mol% CoO were placed inside an alumina sample chamber of the dilatometer (Model 402 E. Netzsch) and sintered at a constant heating rate of 10°C/min in the 30–1400°C temperature range. The variation of the sample length with temperature was detected by a LVDT sensor and stored in a computer for further analysis. Apparent densities have been measured using the Archimedes method.

For impedance spectroscopy measurements the opposite faces of the cylindrical pellets with different compositions were painted with Demetron 308A platinum paste. The samples were placed in an alumina sample chamber with spring-loaded Pt terminal leads. A Pt/Pt–13% Rh thermocouple was used for temperature control and measurements from 30 to 1250°C. In situ impedance spectroscopy analysis (50 mV injected ac voltage signal) was carried out while

the specimen was heated at 10°C/min in the sample chamber inside a programmable tubular furnace. Values of the real (Z') and the imaginary (Z'') parts of the impedance were collected in the 5 Hz–13 MHz frequency range using a Hewlett-Packard 4192A LF impedance analyzer connected via HPIB to an HP 900 controller. IS measurements were also carried out in the sintered specimen during cooling.

3. Results and discussion

Fig. 1 shows the linear shrinkage versus temperature plots for SnO_2 pellets containing 0.5 to 2.0 mol% of CoO. The onset temperature, i.e. the temperature at which shrinkage starts, depends on the CoO concentration in SnO_2.

The higher the CoO concentration, the lower the onset temperatures in these ceramics. All the SnO_2 pellets with CoO additions sintered in the dilatometer up to 1400°C had densities higher than 99% of the theoretical density. These results and the temperatures for the maximum shrinkage are shown in Table 2.

Fig. 2a, 2b, 2c, 2d and 2e show Arrhenius plots of the dc electrical resistivity of $SnO_2 : m$ mol% CoO for $m = 0.5$, 1.0, 2.0, 4.0 and 6.0, respectively. The resistivity values were determined by taking, in the

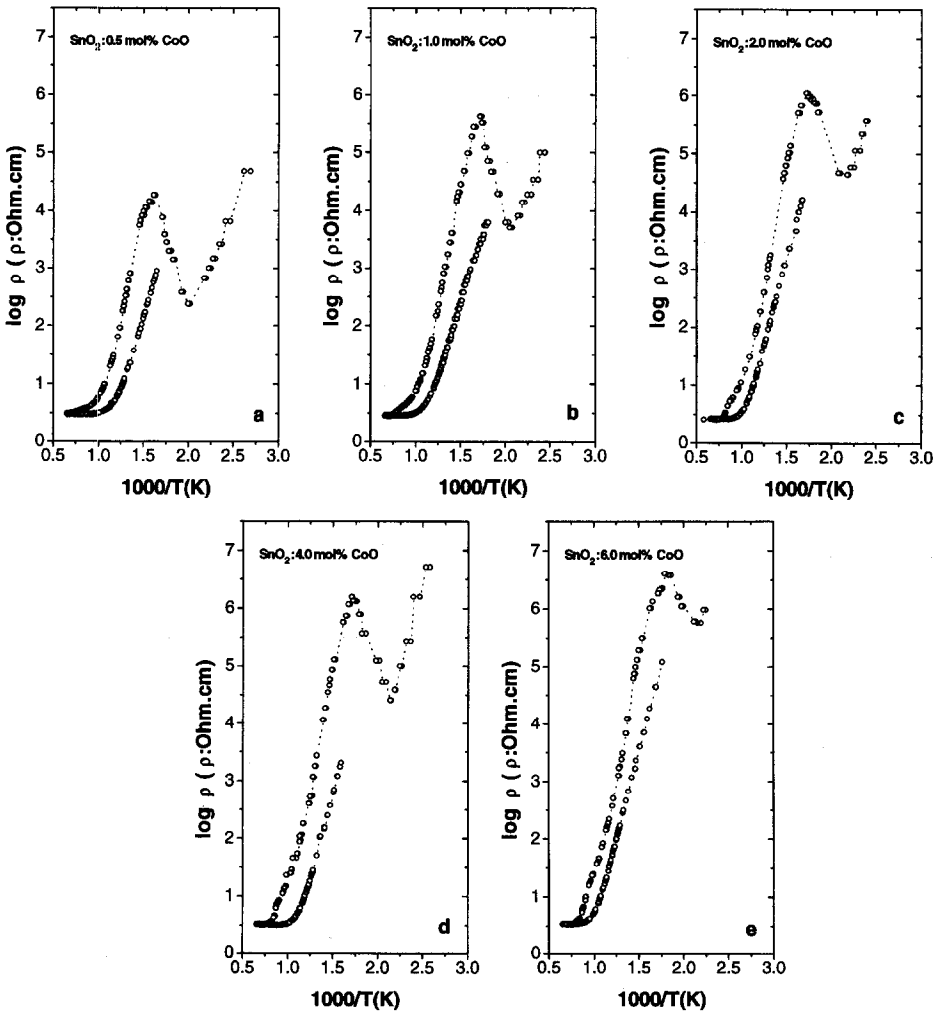

Fig. 2. Arrhenius plots of the electrical resistivity of $SnO_2 : m$ mol% CoO ($m = 0.5$, 1.0, 2.0, 4.0 and 6.0) during sintering at a constant heating rate of 10°C/min up to 1250°C (upper curve) and during cooling (lower curve).

Table 2
Maximum shrinkage temperatures (T_D) of SnO_2:CoO and relative apparent densities (d) of sintered SnO_2:CoO pellets

Sample	T_D (°C)	d (%TD)
SnO_2 + 0.5 mol% CoO	1240	99.4
SnO_2 + 1.0 mol% CoO	1140	99.5
SnO_2 + 2.0 mol% CoO	1040	99.4

$-Z'' \times Z'$ diagram, the intercept with the real axis at the low frequency region of the diagram and multiplying by the geometrical factor A/t (A is the electrode area and t the specimen thickness). Room temperature resistivities are not plotted because the corresponding resistance values are higher than the detection limit of the experimental setup.

Three main features are observed in the plots of Fig. 2: (a) a decrease of more than four orders of magnitude in the resistivity of the specimens; (b) a pronounced resistivity peak with a maximum in the 300–400°C temperature range corresponding to the release of water adsorbed in the specimens; a behavior already reported [22,23]. It is also shown that the higher the CoO addition, the higher the resistivity value at the water liberation region; (c) a constant low resistivity value for temperatures close to the maximum shrinkage rate. During cooling of the sintered samples, lower resistivity values are obtained probably because the specimen is already sintered and there is no more pore contribution.

The high temperature portion of the resistivity versus temperature results was examined in detail. Fig. 3 shows the same electrical resistivity values shown in Fig. 2 as a function of temperature in the 800–1250°C temperature range.

A detailed analysis shows that the higher the CoO content, the lower is the temperature at which the resistivity values are the same for the increasing and the decreasing branches of the resistivity versus temperature plot. These temperatures are indicated in the

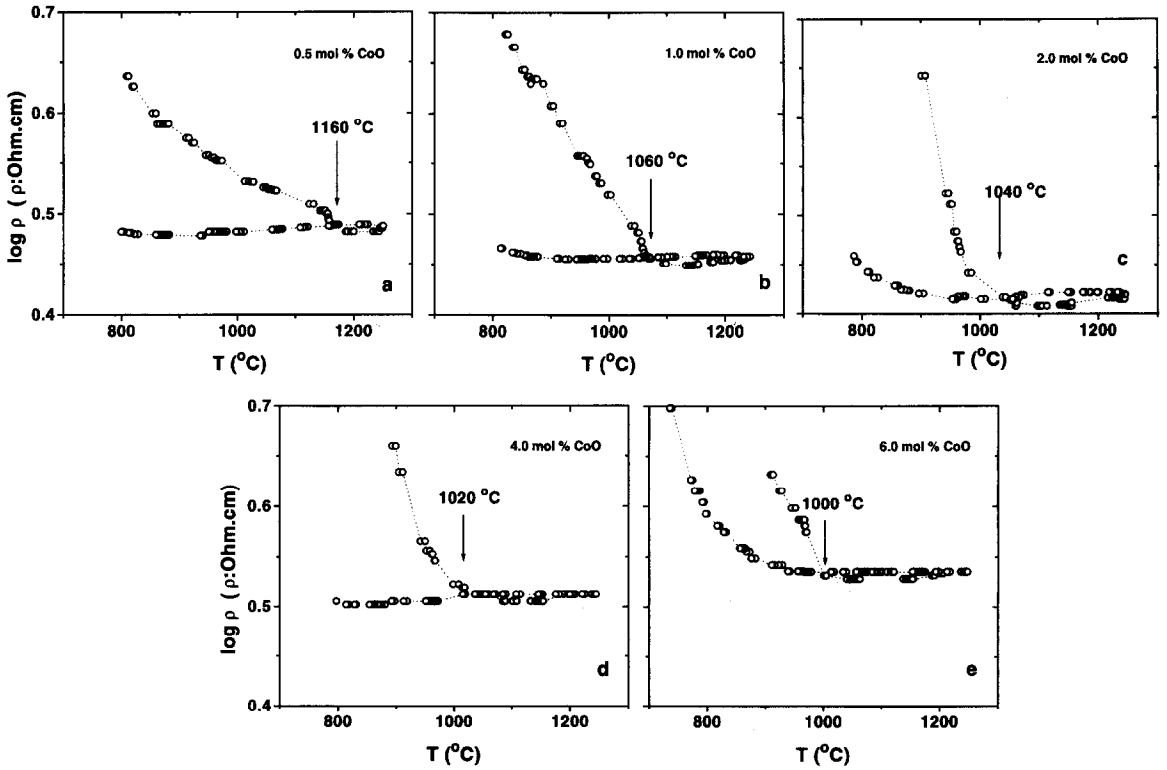

Fig. 3. Electrical resistivity values as a function of temperature of SnO_2 : m mol% CoO (m = 0.5, 1.0, 2.0, 4.0 and 6.0) during sintering at a constant heating rate of 10°C/min in the range 800–1250°C (upper curve) and during cooling (lower curve).

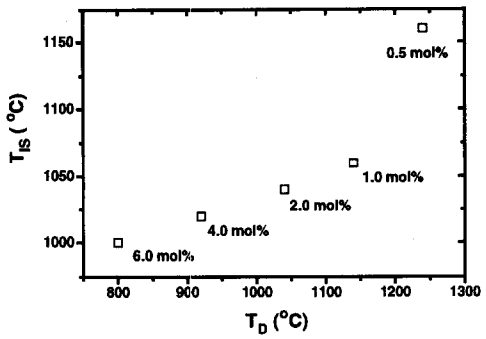

Fig. 4. Maximum shrinkage temperatures (T_D) as a function of the temperature at which the minimum value of resistivity is attained (T_{IS}) in SnO_2 : m mol% CoO for $m = 0.5$, 1.0 and 2.0, 4.0 and 6.0.

figures. The same trend is observed for shrinkage of the samples measured in a dilatometer; that is, the higher the CoO content, the lower the onset temperature for specimen shrinkage (see Fig. 1). The good correlation between the temperatures determined by dilatometry and by impedance spectroscopy is shown in Fig. 4. T_D and T_{IS} stand for the temperatures determined by dilatometry and impedance spectroscopy, respectively.

The constant electrical resistivity behavior of the CoO-doped SnO_2 for temperatures higher than a given sintering temperature (1160°C for SnO_2 + 0.5 mol% CoO) indicates either an ionic conductivity in the liquid or high electronic conductivity path due to electronic defects created by formation of oxygen vacancies. Considering that there is no evidence of liquid phase formation in previous studies [11] and that the constant electrical resistivity behavior still remains during cooling to temperatures well below the shrinkage onset, the observed low resistivity is most probable associated with oxygen vacancy formation due to solid substitution of Sn^{4+} for Co^{2+} ions in the surface of the grains. A high vacancy concentration at the surfaces of the grains would constitute a continuous path for charge carriers through the Co-doped SnO_2 specimens.

4. Conclusions

Impedance spectroscopy analysis during sintering of SnO_2 with CoO additions showed that the higher the amount of the additive, the lower is the temperature at which SnO_2 behaves like an easy path for charge carriers, suggesting that oxygen vacancies are indeed controlling sintering of this oxide. These results are in good agreement with the ones obtained by dilatometry. The impedance spectroscopy technique can then be used to help identify sintering and densification mechanisms in ceramics, provided there are mobile charge carriers in the temperature range where these phenomena occur.

Acknowledgements

We thank Fundação de Amparo a Pesquisa do Estado de São Paulo (FAPESP) and Programa de Apoio ao Desenvolvimento de Ciência e Tecnologia (MCT) for financial support and Y.V. França for the impedance spectroscopy measurements.

References

[1] J.G. Fagan and V.R. Amarakoon, Am. Ceram. Soc. Bull. 72 (1993) 119.
[2] P.P. Tsai, I.C. Chen and M.H. Tzeng, Sensors Actuators B 24–25 (1995) 537.
[3] T.J. Coutts, X. Li and T.A. Cessert, IEEE Electronics Lett. 26 (1990) 660.
[4] T.J. Coutts, N.M. Pearsall and T. Tarricone, J. Vacuum Sci. Technol. B 2 (1984) 140.
[5] P.P. Deimel, B.B. Heimhofer and E. Voges, IEEE Photonic Technol. Lett. 2 (1990) 499.
[6] N. Jakson and J. Ford, Thin Solid Films 77 (1981) 23.
[7] V.G. Panteleev, K.S. Ramm and T.I. Pron'kina, Glass Ceramics 46 (1990) 199.
[8] P. Olivi, E.C.P. Souza, E. Longo, J.A. Varela and L.O.S. Bulhões, J. Electrochem. Soc. 140 (1993) L81.
[9] H.D. Joss, M.Sc. Dissertation, University of Washington (1975).
[10] P.H. Duvigneaud and D. Reighard, in: Science of sintering, Vol. 12, ed. P. Vincenzini (Ceramurgia Srl, Faenza, 1980) p. 287.
[11] J.A. Varela, E. Longo, N. Barelli, A.S. Tanaka and W.A. Mariano, Ceramica 31 (1985) 241.
[12] J.A. Varela, O.J. Whittemore and E. Longo, Ceram. Intern. 16 (1990) 177.
[13] N. Dolet, J.M. Heintz, L. Habardel, M. Onillon and J.P. Bonnet, J. Mater. Sci. 30 (1995) 365.
[14] S.J. Park, K. Hirota and H. Yamamura, Ceramics Intern. 10 (1984) 116.

[15] S. Zuca, M. Terzi and M. Zaharescu, J. Mater. Sci. 26 (1991) 1673.
[16] M. Paria, S. Basu and A. Paul, Trans. Indian Ceram. Soc. 42 (1983) 90.
[17] D.W. Yuan, S.F. Wang, W. Huebner and G. Simkovich, J. Mater. Res. 8 (1993) 1675.
[18] J.A. Cerri, E.R. Leite, D. Gouvea, E. Longo and J.A. Varela, J. Am. Ceram. Soc. 79 (1996) 799.
[19] W.W. Ho and P.E.D. Morgan, J. Am. Ceram. Soc. 70 (1987) C209.
[20] J.-H. Lee, S.-J. Park and K. Hirota, J. Am. Ceram. Soc. 73 (1990) 2771.
[21] J.R. McDonald, ed., Impedance spectroscopy – emphasizing solid materials and systems (Wiley Interscience, New York, 1987).
[22] J.F. McAleer, P.T. Moseley, J.O.W. Norris and D.E. Williams, J. Chem. Soc. Faraday Trans. I 83 (1987) 1323.
[23] C.V. Santilli, S.H. Pulcinelli and A.F. Craievich, Phys. Rev. B 51 (1995) 8801.